International Journal of Signal Processing, Image Processing and Pattern Recognition
Vol.8, No.7 (2015), pp.51-62
http://dx.doi.org/10.14257/ijsip.2015.8.7.06

Image Segmentation Framework Using Gradient Guided Active Contours

Bo Cai[1,2*], Zhigui Liu[2,1], Junbo Wang[2,1] and Yuyu Zhu[2]

1. China Academy of Engineering Physics, Mianyang, Sichuan 621000, China
2. Southwest University of Science & Technology, Mianyang Sichuan 621010, China
caibo_bupt@126.com

Abstract

Image segmentation is a fundamental and challenging problem in image processing and often a vital step for high level analysis. Considering of the inefficient curve evolution against weak boundary and intensity heterogeneous images, an improved level set segmentation framework guided by the image gradient function is proposed. In this framework, the edges and regions of the image are roughly divided by using the image gradient sample function. Compare to the Local Binary Fitting (LBF) model, local and global intensity fitting (LGIF) model, and Edge-flow based active contour model, this algorithm may improve efficient of curve evolution in a large extent. After that, we compare this algorithm with the other active contour model to show that segmenting the noisy blurry boundary and intensity heterogeneous images can be achieved, and still go on an in-depth comparison of these models. Finally, we show the results on challenging images to illustrate the accurate segmentations.

Keywords: *Image segmentation; CV model; Gradient guided function; LBF; LGIF*

1. Introduction

Image segmentation has been the subject of intensive research and a wide variety of segmentation techniques has been reported in recent decades. Active Contour Model (ACM) based segmentation algorithm has been widely investigated and applied to the image segmentation [1-8]. In general, the basic idea of active contour model is to deform an initial contour toward the actual boundary of the object.

In fact, Active Contour Model may be categorized into edge-based [3, 9] and region based [1, 5-6, 10-11] models. In edge and region based ACM, image gradient and statistical information are used to stop the contours respectively. The benefit of the model is that the image has no global constraints, thus the objective and the background can be heterogeneous and the final segmentation can be got easily. However, the method relies heavily on edge information of the input image, when an edge of the region is weak, such as blurred, or broken, the method may loss its roll.

Region-based active contour model (ACM) utilizes the objective and the background regions statistically and finds an energy optimum where the model best fits the image. Because of more advantages over edge-based ACMs, such as robustness for image with weak edges or without edges and insensitivity to the location of initial contours, region-based ACMs have been applied more popularly, in which, the Chan-Vese (CV) model [12] is one of the most popular region-based models. However, techniques that attempt to model regions using these kinds of methods are usually not ideal for segmenting heterogeneous objects, or transitional regions, which frequently occur in natural images.

ISSN: 2005-4254 IJSIP

According to the above analysis, a good active contour based segmentation model should consider the advantages of edge-based and region-based information to segment the image accurately. There are many methods in the literature which are aimed at improving the segmentation accurate by introducing more edge or region information into the active contour model. Because of the minimization of the energy function heavily depends on the gray scale and region distribution of the image, the total information often leads to the false segmentation in the local region of the image. To overcome the problem of region non-homogeneous, Ge Qi *et al.* [11] proposed a region based model with an anisotropic region fitting energy represented by a variational energy functional. They introduced a structure tensor to define an anisotropic region fitting energy functional so that the intensity of an observed pixel is approximated through the intensity of its adjacent pixels at the principal directions. For the purpose of letting the active contour model more conform to the edges of the image region, Kovacs, Andrea *et al.* [13] generates the main feature points based on the Harris corner detector, then these points are enveloped to get the initialization of the contour. Faced on the problems of intensity inhomogeneity, Yang, Yunyun *et al*. [14] divide the fitting energy as local intensity fitting (LIF) energy and global intensity fitting (GIF) energy, and then use the two terms RSF model and CV model to realize the minimization of local-global intensity energy function. Since the external force plays a leading role in driving the active contour models, designing a novel external force field has been extensively studied [1, 5, 9-10, 15]. Among all these external forces, gradient, edge, and gradient vector flow (GVF) has been used by Zhou Huiyu *et al*. [16] as the outer driven force. In [9], Fang Lingling *et al*. using the EdgeFlow-Based (EFB) active contour to realize the segmentation of the heterogeneous regions. Because of the edge of the regions is difficult to get, they use the Gaussian Mixture Model to realize the initial contour.

In this paper, considering of the inhomogeneous of the regions and edges of the image region, we focus on the edge detection of the image regions. Based on the Edge-Flow model [9], an adjusted active contour model has been proposed in this paper. Based on this model, we study in depth the effect of the different gradient guided function on segmentation results. After the comparison of different gradient algorithms including the normal gradient modulus function, the wavelet modulus function, and the simple gradient vector function, we proposed a new gradient calculate algorithm which may more efficient to avoid the double edges, and efficient to detect the weak object boundaries. Finally, we provide a way for initializing active contours: global contrast and local gradient based initialization model. This method creates an initial active contour, which may reduce the computational complexity, and make the result close to the object boundary.

The remainder of this paper is organized as follows. In Section 2, we give briefly review the CV and some other ACM based models. The proposed model is introduced in Section 3. In Section 4, the role of different gradient algorithm has been compared in our proposed model. Section 5 is the comparison of our model with LGIF, LBF, and EFB (Edge-flow based ACM) in evolution efficient and segmentation results. We go on analyzing the results when the image is noised. Finally, the conclusion and limitations of our model have been discussed in Section 6.

2. The Review and Discussion of the Related Works

In this section, we give a review of the related outer driving models based on Chan and Vese [12] model. For a given image $I(x)$ on the image domain R, Chan-Vese propose to minimize the following energy equation:

$$E^{CV}\left(c_1,c_2,C\right)=\lambda_1\int_{in(C)}\left|I\left(x\right)-c_1\right|^2dx+\lambda_2\int_{out(C)}\left|I\left(x\right)-c_2\right|^2dx \tag{1}$$

where c_1 and c_2 are two constants that approximate the average intensity inside and outside the curve, respectively. The coefficients λ_1 and λ_2 are fixed parameters.

In Chan-Vese model, they also have a regularizing term, such as the length of the contour and the area inside and outside the contour to improve the smoothness of the boundary. The energy $E^{CV}\left(c_1,c_2,C\right)$ is defined as：

$$\begin{aligned}E^{CV}\left(c_1,c_2,C\right)&=\lambda_1\int_{in(C)}\left|I\left(x\right)-c_1\right|^2dx+\lambda_2\int_{out(C)}\left|I\left(x\right)-c_2\right|^2dx\\&+\mu\mathrm{L}ength\left(C\right)+\nu Area\left(in\left(C\right)\right)\end{aligned} \tag{2}$$

Using the level set to represent C, that is, C is the zero level set of Lipschitz function $\phi\left(x\right)$, the energy function may be rewritten as:

$$\begin{aligned}E^{CV}\left(c_1,c_2,\phi\right)&=\lambda_1\int_{\mathrm{R}}\left|I\left(x\right)-c_1\right|^2H\left(\phi\left(x\right)\right)dx+\lambda_2\int_R\left|I\left(x\right)-c_2\right|^2\left(1-H\left(\phi\left(x\right)\right)\right)dx\\&+\mu\int_R\delta\left(\phi\left(x\right)\right)\left|\nabla\phi\left(x\right)\right|dx+\nu\int_R H\left(\phi\left(x\right)\right)dx\end{aligned} \tag{3}$$

where $H\left(\phi\right)$ and $\delta\left(\phi\right)$ are Heaviside function and Dirac function, respectively.

The CV model has a good performance on image segmentation due to its ability of obtaining a larger convergence range and being less sensitive t the initialization. However, the CV model is only adapted for 2-phase image. If the intensities with inside C or outside C are not homogeneous, the constants c_1 and c_2 will not be accurate. To overcome the difficult caused by intensity inhomogeneous, Li et al. proposed the local binary fitting (LBF) model[17], which can utilize the local intensity information. In the LBF model, two spatially varying fitting functions $f_1\left(x\right)$ and $f_2\left(x\right)$ are introduced to approximate the local intensities on the two sides of the contour, and for a given point $x\in R$, the local intensity fitting energy is defined by

$$\begin{aligned}E_x\left(C,f_1,f_2\right)&=\lambda_1\int_{in(C)}g\left(x-y\right)\left(I\left(y\right)-f_1\left(x\right)\right)^2dy\\&+\lambda_2\int_{out(C)}g\left(x-y\right)\left(I\left(v\right)-f_2\left(x\right)\right)^2dy\end{aligned} \tag{4}$$

where λ_1 and λ_2 are positive constants, $\mathrm{g}\left(y\right)$ is a Gaussian kernel function, and $f_1\left(x\right)$, $f_2\left(x\right)$ are two values that approximate image intensity inside and outside contour C, respectively.

The above local fitting energy $E_x\left(C,f_1,f_2\right)$ is defined for a center point x. For all the center point x in the image domain R, the energy function can be defined by

$$\begin{aligned}E^{LBF}\left(C,f_1\left(x\right),f_2\left(x\right)\right)&=\int_R E_x\left(C,f_1\left(x\right),f_2\left(x\right)\right)dx\\&=\lambda_1\int_R\left[\int_R g\left(x-y\right)\left(I\left(y\right)-f_1\left(x\right)\right)^2H\left(\phi\left(y\right)\right)dy\right]dx\\&+\lambda_2\int_R\left[\int_R g\left(x-y\right)\left(I\left(v\right)-f_2\left(x\right)\right)^2\left(1-H\left(\phi\left(y\right)\right)\right)dy\right]dx\end{aligned} \tag{5}$$

Another way to deal with the intensity discontinuity is use the edge information as the factor of the ACM model. Fang *et al.* [18] define the energy function $x\in R$ as

$$\begin{aligned} E_x^{EFB} &= \int_{in(C)} g(y)\left|I(y)-c_1\right|^2 dy + \int_{out(C)} g(y)\left|I(y)-c_2\right|^2 dy + \lambda\int_R \delta_\varepsilon\left(\phi(x)\right)\left|\nabla\phi(x)\right| \\ &= \int_R g(y)\left|I(y)-c_1\right|^2 H_\varepsilon(\phi)\,dy \\ &+ \int_R g(y)\left|I(y)-c_2\right|^2 \left(1-H_\varepsilon(\phi)\right)dy \\ &+ \lambda\int_R \delta_\varepsilon\left(\phi(x)\right)\left|\nabla\phi(x)\right| \end{aligned} \tag{6}$$

where $g(y)$ denotes Edge-Flow Based function: $g(y)=1\Big/\left(1+\left(y/k\right)^2\right)^m$, k is a contrast parameter separating low-contrast regions from high-contrast edges: $K=1.4826\times median\left(\left\|y-median(y)\right\|\right)$. They define $median(\cdot)$ as median operation, and use this selective process ensures that the image operation. And this selective process ensures that the image region is for $y<k$ and the image edge is for $y\geq$ k . Besides, m is a regulatory factor of Edge-Flow based function, which can achieve a better balance between keeping edge and removing the noise near the edge.

Following this way, there are some papers aimed at dividing the local characters and the global characters of the image [3-5, 15, 19-20], and constructing the energy function to solve the global and local problems. In this paper, we'll following the visual processing of the image to deal with the local and problems. As stated in [18], the global contrast and local contrast is the key reference in human visual processing. Commonly, the contrast of image is related to the edge of the image regions. However, the edges are often exists in the different phase of image regions, and make the edges inhomogeneous in local regions. Simply sum the difference of all local regions may cause the global optimizing function result inconsistence to the local dividing results. On the other hand, only using the local dividing result to approximate the global segmentation may cause the wrong segment of the transitional regions and the parameter is difficult to choose.

3. The Proposed Model

In this paper, we focus on the role of the image gradient and the global/local contrast in the active contour model (ACM) iteration. According to our experiments, the global mean c_1 and c_2 is the classification center of the image gray, and their value are mainly influenced by the total inner region pixels instead of the edge pixels. Comparing to the inner gray distribution, the contour is more easily influenced by the edge pixels' gray. At the same time, because of the inhomogeneous of the region edges, the dividing of different region may exist or not exist in the difference between c_1 and c_2. When the edge-grays of the region are all less than or bigger than the global center c_1 and c_2, the global dividing reference may lose its role.

Given the input image $I(x)$ on the image domain R, Chan-Vese proposed to minimize the energy function as eq.1. For the purpose of letting the region inner area and region edges play roles efficiently, we consider the edge factor in the iteration processing of ACM model, and then redefining the energy function with respect to the edge information.

$$\begin{aligned} E^{CV}(c_1,c_2,C) &= \lambda_1\int_R \left|I(x)-c_1\right|^2 H\left(\phi(x)\right)dx + \lambda_2\int_R \left|I(x)-c_2\right|^2\left(1-H\left(\phi(x)\right)\right)dx \\ &+ \mu\int_R \delta\left(\phi(x)\right)\left|\nabla\phi(x)\right|dx + \nu\int_R H\left(\phi(x)\right)dx \end{aligned} \tag{7}$$

where $H(\phi)$ and $\delta(\phi)$ are Heaviside function and Dirac function respectively. Generally, the regularized versions are selected as

$$H_\varepsilon(z)=\frac{1}{2}\left(1+\frac{2}{\pi}\arctan\left(\frac{z}{\varepsilon}\right)\right)$$
$$\delta_\varepsilon(z)=\frac{1}{\pi}\frac{\varepsilon}{\varepsilon^2+z^2},\quad z\in R \tag{8}$$

In Chan-Vese model, they keep the $\phi(x)$ fixed, and minimizing the energy $E^{CV}(c_1,c_2,\phi)$ with respect to the constant c_1 and c_2 as

$$\begin{cases} c_1(\phi)=\dfrac{\int_R I(x)H(\phi(x))dx}{\int_R H(\phi(x))dx} \\ c_2(\phi)=\dfrac{\int_R I(x)(1-H(\phi(x)))dx}{\int_R (1-H(\phi(x)))dx} \end{cases} \tag{9}$$

Here, c_1 and c_2 are the means of the foreground and background of the image. For the purpose of letting region information guide the iteration, we divide the image into two parts as region inner area and region edge area. Before the calculation of the background mean and foreground mean, we use the Gaussian function to resample the region inner pixels of $\phi(x)$ as

$$\begin{cases} c_1'(\phi)=\dfrac{\int_R I(x)H(g_k(x)\phi(x))dx}{\int_R H(g_k(x)\phi(x))dx} \\ c_2'(\phi)=\dfrac{\int_R I(x)(1-H(g_k(x)\phi(x)))dx}{\int_R (1-H(g_k(x)\phi(x)))dx} \end{cases} \tag{10}$$

where $g_k(x)=1/\sqrt{2\pi}\exp(-x^2/2\sigma^2)$ is the Gaussian sampling kernel function. After the resampling processing, we keep c_1' and c_2' fixed, and then to minimize the energy function $E^{CV}(c_1,c_2,\phi)$ with respect to $g(x)\phi(x)$. Parameterizing the descent direction by an artificial time t, we can obtain the corresponding variational level set function as follows:

$$\begin{cases} \dfrac{\partial\phi'(x,t)}{\partial t}=\delta(\phi')\left[-\lambda_1(I(x)-c_1')^2+\lambda_2(I(x)-c_2')^2+\mu div\left(\dfrac{\nabla\phi'}{|\nabla\phi'|}\right)-\upsilon\right] \\ \phi'(x)=g_k(x)\phi(x) \end{cases} \tag{11}$$

For the sampling of the inner regions, we simply use the mean gradient to dividing the image into region inner and region edge as

$$\begin{cases} \mathrm{Re}\,gion_{inner}=\{Grad(x)<=Mean(Grad(x)),x\in R\} \\ \mathrm{Re}\,gion_{edge}=\{Grad(x)>Mean(Grad(x)),x\in R\} \end{cases} \tag{12}$$

where $Grad(x)$ is the gradient of the image pixel x, $x\in R$. In this step, we let the region edge pixels in normal steps as eq.7. For more accurate computation involving the level set function and its evolution, we regularize the level set function by penalizing its deviation from signed distance function. At the same time, we also have a regularizing the

length of C to control the smoothness of the boundary. The two terms can be characterized by the following energy function:

$$E^R(\phi) = \mu\int_R \delta(\phi(x))|\nabla\phi(x)|)dx + \nu\int_R (|\nabla\phi(x)|-1)dx \tag{13}$$

Therefore, we can define the total energy function:

$$\begin{aligned} E^{CV}(c_1', c_2', C) &= \lambda_1\int_R |I(x)-c_1'|^2 H(\phi'(x))dx + \lambda_2\int_R |I(x)-c_2'|^2 (1-H(\phi'(x)))dx \\ &+ \mu\int_R \delta(\phi'(x))|\nabla\phi'(x)|dx + \nu\int_R H(\phi'(x))dx \end{aligned} \tag{14}$$

Because of using the image gradient in the iteration processing, specifically the region inner pixels, the iteration processing is able to make the region inner pixels more smooth, and at the same time accelerate the evolution. As a result, because of the resampling of the inner region, it makes the energy more similar to the region contour, the time – consumption is also heavily decreased.

4. Various Gradient Measures

Having formulated our model of iteration processing, we give the discussion of the different gradient measures. Commonly, the simple Gradient Vector function, the normal Gradient Modulus function, and the Wavelet Modulus function are used as the Gradient calculating functions.

The simple image gradient is to compute a directional change in the intensity of the image. Each pixel of a gradient image measures the change in intensity of te same point in the original image and in a given direction. T get the full range of direction, the gradient image in the i and j directions of point x is computed as the formula:

$$\nabla f = \frac{\partial f}{\partial i}, \frac{\partial f}{\partial j} \tag{15}$$

where $\partial f/\partial i$ and $\partial f/\partial j$ are the gradients in the i and j directions, respectively. The gradient magnitude and the gradient direction can be calculated by

$$\begin{cases} |\nabla f| = \sqrt{\left|\frac{\partial f}{\partial i}\right|^2 + \left|\frac{\partial f}{\partial j}\right|^2} \\ \theta = \arctan\left(\left|\frac{\partial f/\partial j}{\partial f/\partial i}\right|\right) \end{cases} \tag{16}$$

This function is simplicity of the computation, and more desirable than the others when the image has obvious edge and continuous intensity. However, once the image has intangible information, this method will reduce in its workability.

In response to the above problem, the smoothing on both sides of an edge is much stronger than smoothing across it, which will keep the edge of the image information better. The Gaussian filtering in the i and j direction of point x is computed by the formula:

$$f(i,j) = \frac{1}{2\pi MN}\sum_{m=1}^{M}\sum_{n=1}^{N} K(i-m)K(j-n)I(m,n) \tag{17}$$

where $K(x) = 1/\sqrt{2\pi}\exp(-x^2/2\sigma^2)$, and σ is the variance, M, N is the size of the image. The partial derivative of $f(i,j)$ is expressed as

$$\begin{cases} f_i = \dfrac{1}{2\pi MN}\sum_{n=1}^{N} K(j-n)\left\{\sum_{m=1}^{M} K'(i-m)I(m,n)\right\} \\ f_j = \dfrac{1}{2\pi MN}\sum_{m=1}^{M} K(i-m)\left\{\sum_{n=1}^{N} K'(j-n)I(m,n)\right\} \end{cases} \tag{18}$$

The variance between the original image and the Gaussian filtered image is:

$$D^2 = \frac{1}{MN}\sum_{m=1}^{M}\sum_{n=1}^{N}\left(I(m,n) - f(m,n)\right)^2 \tag{19}$$

The covariance of (f_i, f_j) is:

$$\sum(i,j) = \begin{pmatrix} \sigma_{11}(i,j) & \sigma_{12}(i,j) \\ \sigma_{21}(i,j) & \sigma_{22}(i,j) \end{pmatrix} \tag{20}$$

where

$$\begin{cases} \sigma_{11}(i,j) = \dfrac{D^2}{4\pi^2 M^2 N^2}\sum_{m=1}^{M}\sum_{n=1}^{N} K^2(j-n)K'^2(i-m) \\ \sigma_{22}(i,j) = \dfrac{D^2}{4\pi^2 M^2 N^2}\sum_{m=1}^{M}\sum_{n=1}^{N} K^2(i-m)K'^2(j-n) \\ \sigma_{12}(i,j) = \dfrac{D^2}{4\pi^2 M^2 N^2}\sum_{m=1}^{M}\sum_{n=1}^{N} K(i-m)K'(i-m)K(j-n)K'(j-n) \end{cases} \tag{21}$$

The standard gradient is defined as

$$\begin{aligned} G_s(x) &= G_s(i,j) \\ &= \frac{f_i^2(i,j)\sigma_{22}(i,j) + f_j^2(i,j)\sigma_{11}(i,j) - 2\sigma_{12}(i,j) f_i(i,j) f_j(i,j)}{\sigma_{11}(i,j)\sigma_{22}(i,j) - \sigma_{12}^2(i,j)} \end{aligned} \tag{22}$$

Let $\theta(i,j)$ be a 2D differentiable smoothing function whose integral is 1 and converges 0 at infinity. The two oriented wavelets can be constructed by teking the first-order derivative of $\theta(i,j)$:

$$\begin{cases} \psi^{(1)}(i,j) = \dfrac{\partial\theta(i,j)}{\partial i} \\ \psi^{(2)}(i,j) = \dfrac{\partial\theta(i,j)}{\partial j} \end{cases} \tag{23}$$

The wavelet translation (WT) of image $I(x)$ at dyadic scale $a = 2^b$, $(b \in Z)$ is

$$\begin{cases} WT_a^{(1)} I(x) = I(x) * \psi_a^{(1)}(i,j) \\ WT_a^{(2)} I(x) = I(x) * \psi_a^{(2)}(i,j) \end{cases} \tag{24}$$

where $*$ denotes convolution operation, further, the vector form os the above equation:

$$\begin{bmatrix} WT_a^{(1)} I(x) \\ WT_a^{(2)} I(x) \end{bmatrix} = a\begin{bmatrix} \dfrac{\partial\left(I(x) * \theta_a(i,j)\right)}{\partial x} \\ \dfrac{\partial\left(I(x) * \theta_a(i,j)\right)}{\partial y} \end{bmatrix} = a\,grad\left(I(x) * \theta_a(i,j)\right) \tag{25}$$

Consider the local maximum of the gradient magnitude and gradient direction at various scales given by

$$\begin{cases} M_a f(x) = \sqrt{\left|WT_a^{(1)} f(x)\right|^2 + \left|WT_a^{(2)} f(x)\right|^2} \\ A_a f(x) = \arctan\left[\dfrac{WT_a^{(2)} f(x)}{WT_a^{(1)} f(x)}\right] \end{cases} \tag{26}$$

Combining the similarity and discontinuity (low-pass and high-pass) into a signal approach effectively, the method can form a multi-scale edge representation of an image.

In this paper, considering of the time-consumption and the stability of the image gradient, we choose the simple gradient algorithm. Unlike the directly calculate of the gradient, we use the Gaussian kernel function g_k and the mean template g_m as the filter to deal with the image gradient firstly, and then calculate the magnitude of the image gradient as

$$\nabla f = \max\left\{abs\left(\frac{\partial f}{\partial i}\right), \text{abs}\left(\frac{\partial f}{\partial j}\right)\right\} \tag{27}$$

$$\nabla f' = \left\{\nabla f_k(x) - \nabla f_m(x) \geq 0, x \in R\right\}$$

$$\nabla f_k(x) = g_k \nabla f \tag{28}$$

$$\nabla f_m(x) = g_m \nabla f$$

where g_k is the Gaussian kernel function, g_m is the mean template. For all the template size, we choose 5×5 in our experiments. After the calculating of the gradient, $\nabla f'$ is chosen as the guided gradient of our model. Figure 1 shows the calculating results.

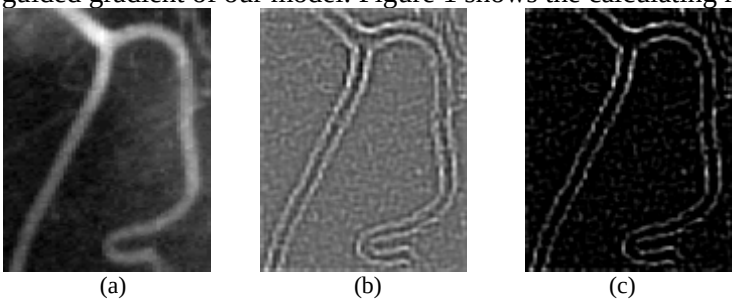

(a) (b) (c)

Figure 1. The Rough Image, the Image Gradient and the Guided Image Gradient

5. Experimental Results

In order to demonstrate the strengths of the proposed model, we perform different kinds of experiments. First of all, we compare the proposed model segment results with the other local based ACM model such as LBF, LGIF, and Edge-Based active contour model. Secondly, we continue with the properties of the proposed model with various images, and analyze the corresponding number of iterations and time. Finally, so we'll give the analysis of the guided gradient extraction with different coefficients.

Commonly, the accurate choose of initial contour is an important part in the process of image segmentation. In our model, the resampling of the inner region has the ability of dealing with the wrongly initialize contour, as a result, it may leads the iteration convergence to the correct edge of the image. Firstly, we will give the comparison of the different initial contour of different algorithms. In this experiment, we choose two kinds of initial contours (the edge included initial contour and none edge initial contour) by hand. For the iteration times, we set it as 300. Figure 2 and Figure 3 show the results of the proposed model, LGIF, LBF, and LCV with different initial contour.

Figure 2. The iteration results of different our model and the other local based models with the initial contour on the region edge, the first column is the proposed model, the second column is the result of LBF, the third column is the result of LCV, and the last column is the result of LGIF.

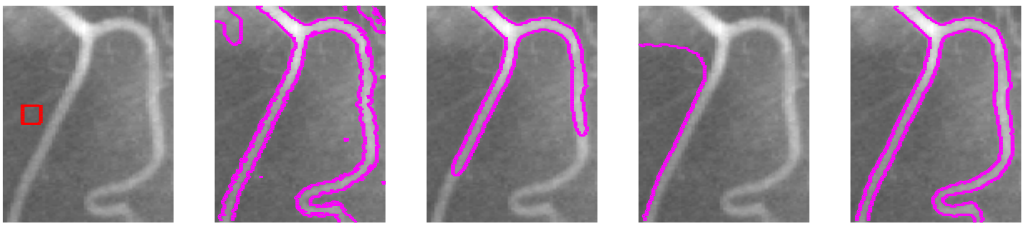

Figure 3. The iteration results of different our model and the other local based models with the initial contour is not on the region edge, the first column is the proposed model, the second column is the result of LBF, the third column is the result of LCV, and the last column is the result of LGIF.

In this part, we give compare the corresponding energy value of the proposed algorithm and the other local based active contour models. For the purpose of compare the convergence of the energy values, we scale the total energy and give the curve of different models. Because of the initial contour of different model may causing different results, we choose the correct initial contour with different model to compare the convergence.

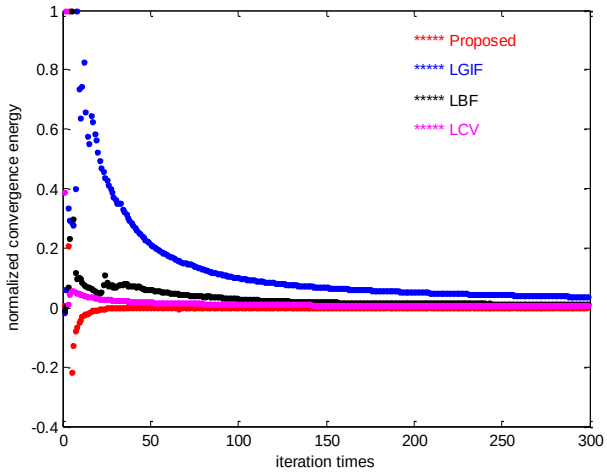

Figure 4. The Comparison of the Convergence of Different Algorithms

Like all of the active contour based segmentation models, the parameter of our model is also an important problem. In our algorithm, the image are roughly divided into two region inner pixels and region edge pixels, but the choosing of the threshold between the different gradients is very difficult. The fix value would not fit different input images. For the purpose of letting the algorithm more adaptable, the dividing of the gradient should be adjusted according to the input image, or even based on the different image regions. In the following works, the study of the local adaptable dividing would be our main works.

Figure 5. The Segmentation Results

6. Conclusion

In this work, we propose a novel framework based on active contour model for image segmentation. The proposed model may efficiently utilizes image gradient and region information, which in certain case has resulted in significant improvement in accuracy and time consuming for segmenting various images with multi-phase object boundaries.

Like all of the active contour based segmentation models, the parameter of our model is also an important problem. In our algorithm, the image are roughly divided into two region inner pixels and region edge pixels, but the choosing of the threshold between the different gradients is very difficult. The fix value would not fit different input images. For the purpose of letting the algorithm more adaptable, the dividing of the gradient should be adjusted according to the input image, or even based on the different image regions. In the following works, the study of the local adaptable dividing would be our main works.

Acknowledgements

The authors thank the anonymous reviewers for their many valuable comments and suggestions that helped to improve both the technical content and the presentation quality of this paper.

References

[1] Q. Zheng, E. Dong, Z. Cao, W. Sun, and Z. Li, “Active contour model driven by linear speed function for local segmentation with robust initialization and applications in MR brain images”, *Signal Processing*, vol. 97, (**2014**), pp. 117-133.
[2] W. Wang, L. Zhu, J. Qin, Y.-P. Chui, B. N. Li, and P.-A. Heng, “Multiscale geodesic active contours for ultrasound image segmentation using speckle reducing anisotropic diffusion”, *Optics and Lasers in Engineering*, vol. 54, (**2014**), pp. 105-116.
[3] Q. Zheng and E.-Q. Dong, “Narrow Band Active Contour Model for Local Segmentation of Medical and Texture Images," *Acta Astronautica Sinica*, vol. 39, (**2013**), pp. 21-30.
[4] X. Xie, J. Wu, and M. Jing, "Fast Two-Stage Segmentation via Non-Local Active Contours in Multiscale Texture Feature Space," *Pattern Recognition Letters*, vol. 34, (**2013**), pp. 1230-1239.
[5] Y. Wu, Y. Wang, and Y. Jia, "Adaptive diffusion flow active contours for image segmentation," *Computer Vision and Image Understanding*, vol. 117, (**2013**), pp. 1421-1435.
[6] D. Li, W. Li, and Q. Liao, "Active contours driven by local and global probability distributions," *Journal of Visual Communication and Image Representation*, vol. 24, (**2013**), pp. 522-533.
[7] L. Wang, C. Li, Q. Sun, D. Xia, and C.-Y. Kao, "Active contours driven by local and global intensity fitting energy with application to brain MR image segmentation," *Computerized medical imaging and graphics*, vol. 33, no. 7, (**2009**), pp. 520-531.
[8] S. Lankton and A. Tannenbaum, "Localizing region-based active contours," *Image Processing, IEEE Transactions on*, vol. 17, (**2008**), pp. 2029-2039.
[9] L. Fang and X. Wang, "Image segmentation framework using EdgeFlow-Based active contours," *Optik - International Journal for Light and Electron Optics*, vol. 124, (**2013**), pp. 3739-3745.
[10] W. Liu, Y. Shang, and X. Yang, "Active contour model driven by local histogram fitting energy," *Pattern Recognition Letters*, vol. 34, (**2013**), pp. 655-662.
[11] Q. Ge, L. Xiao, H. Huang, and Z. H. Wei, "An active contour model driven by anisotropic region fitting energy for image segmentation," *Digital Signal Processing*, vol. 23, (**2013**), pp. 238-243.
[12] T. F. Chan and L. A. Vese, "Active contours without edges," *Image Processing, IEEE Transactions on* vol. 10, (**2001**), pp. 266-277.

[13] A. Kovacs and T. Sziranyi, "Harris function based active contour external force for image segmentation," *Pattern Recognition Letters*, vol. 33, (**2012**), pp. 1180-1187.
[14] Y. Yang and B. Wu, "Split Bregman method for minimization of improved active contour model combining local and global information dynamically," *Journal of Mathematical Analysis and Applications*, vol. 389, (**2012**), pp. 351-366.
[15] C.-y. Yu, W.-s. Zhang, Y.-y. Yu, and Y. Li., "A novel active contour model for image segmentation using distance regularization term," *Computers & Mathematics with Applications*, vol. 65, (**2013**), pp. 1746-1759.
[16] H. Zhou, X. Li, G. Schaefer, M. E. Celebi, and P. Miller, "Mean shift based gradient vector flow for image segmentation," *Computer Vision and Image Understanding*, vol. 117, (**2013**), pp. 1004-1016.
[17] Z. Liu, L. Shen, and Z. Zhang, "Unsupervised image segmentation based on analysis of binary partition tree for salient object extraction," *Signal Processing*, vol. 91, (**2011**), pp. 290-299.
[18] J.-W. Han, Suryanto, J.-H. Kim, S. Sull, and S.-J. Ko, "New edge-adaptive image interpolation using anisotropic Gaussian filters," *Digital Signal Processing*, vol. 23, (**2013**), pp. 110-117.
[19] L. Wang and C. Pan, "Robust level set image segmentation via a local correntropy-based K-means clustering," *Pattern Recognition*, vol. 47, (**2014**), pp. 1917-1925.
[20] V. Kumar, J. K. Chhabra, and D. Kumar, "Automatic cluster evolution using gravitational search algorithm and its application on image segmentation," *Engineering Applications of Artificial Intelligence*, vol. 29, (**2014**), pp. 93-103.

Authors

Bo Cai, he received his B.S. degree in mechatronics from China Agricultural University, in 1998, and M.S degree in Beijing University of Posts and Telecommunications, in 2003. Currently, he is the Ph.D. candidate of China Academy of Engineering Physics. His research interests include image processing and detection.

Zhigui Liu, he received the Ph.D. degree in traffic information engineering and control from Southwest Jiao Tong University, China, in 2006. Currently, he is the teacher of Southwest University of Science & Technology, and Ph. D tutor of China Academy of Engineering Physics. His research interests include vision sensor technology, image processing and machine vision, etc.

Junbo Wang, he received his B.S. degree in physics from Sichuan Normal University, China, in 1981, and the Ph.D. degree in optical engineering from Chengdu electronic science and technology University, China, in 1985. Currently, he is the teacher of Southwest University of Science & Technology, and Ph. D tutor of China Academy of Engineering Physics. His research interests include atmospheric optical and detection, etc.

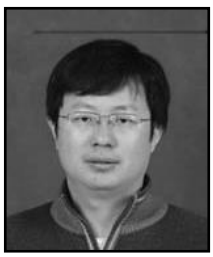

Yuyu Zhu, he received his B.S. degree in automation from Southwest University of Science & Technology, in 2002, and M.S degree in control engineering and control theory, in 2009. Currently, he is the teacher of Southwest University of Science & Technology. His research interests include signal detection and processing, power designing etc.